Visualizing visual impairments

M.A. Hogervorst
TNO Human Factors, Kampweg 5, 3769 DE Soesterberg, the Netherlands
E: maarten.hogervorst@tno.nl

W.J.M. van Damme
Sensis, Javastraat 104, 6524 MJ Nijmegen, the Netherlands

M.A. Hogervorst, W.J.M. van Damme, Visualizing visual impairments. Gerontechnology 2006; 5(4):208-221. We developed and evaluated methods to visualize the limitations of visually impaired persons. Three types of simulation were developed: (i) fixation independent, showing which elements remain visible after ample inspection, related to object recognition, (ii) fixation dependent, showing which elements remain visible in the entire visual field while fixating one part of the image, related to search, and (iii) the effect of glare, an important factor of low vision in for instance cataract patients. In experiments with impaired and unimpaired subjects we determined the extent to which a natural image can be blurred before it can be discriminated from the original, and how this is linked to Landolt-C visual acuity. The relationship between blur threshold and minimum angle of resolution was found to be independent of the cause of reduced vision: visual impairment, reduced contrast, or eccentric viewing. Based on this finding we propose a fixation independent simulation in which the local blur varies with local contrast, linked by the subject's contrast sensitivity function. The fixation dependent simulation type is derived from the peripheral acuity using the relationship between blur threshold and acuity, and perimeter data describing visual field defects. The glare simulation is based on a validated CIE model describing the veiling luminance due to a light source, treating all pixels as independent light sources. These visualizations should give unimpaired persons insight into the problems faced by persons with low vision. The fact that the visualizations are validated by human observer experiments make them suitable for evaluating and adapting designs of architecture, public (road) infrastructure, and products to the needs of the low vision community.

Keywords: impairment, simulation, glare, contrast, acuity, eccentric vision

The goal of our study was to develop methods to visualize the visual limitations of visually impaired persons in order to give unimpaired persons insight into the problems faced by visually impaired people. The visualizations should be a good quantitative description of the main visual limitations and predict performance in important tasks such as object detection and object search for various types of visual impairments; the visualizations can even be tailored to the individual. The visualization methods are partly based on existing knowledge of the visual system and partly based on new experiments.

Due to new technology applications such as internet, cash dispensers, and mobile phones, visual information has become more and more important. Meanwhile, a not negligible proportion of the population (about 1.2% in the Netherlands) is to be registered as 'partially sighted' or blind, and the number is growing every year with demographic developments. Most visual impairments are acquired late in life; about 2% of those suffering from impairments are under the age of 16, 10% between 16 and 59, and 88% over 60 years old[1]. Given the age distribution of the population it can be expected that in countries

similar to the Netherlands the number of visually impaired people will double in the next twenty years. It is therefore increasingly important that both limitations and remaining possibilities of visually impaired people are recognized and taken in consideration when designing products, infrastructure (for instance, road design, crossings), architecture, and so forth.

Various methods can be used to gain insight into the possibilities and limitations of visually impaired people. One way is to use visualizations. An example is the color deficiency simulator developed by Walraven and Alferdinck[2]. Based on knowledge about the sensitivities of the human color receptors and the spectral filtering of the eye lens and macular pigment, specific types of color deficiencies can be simulated. This simulation can be used as a diagnostic design tool and also provides the means for adjusting the colors to the individual needs of specific color-deficient viewers.

A similar simulation tool would be useful for other forms of visual impairments such as in macula degeneration, cataract, glaucoma, and diabetic retinopathy. Here we will present various simulation methods. These are based on quantitative limitations in visual functions, rather than on ophthalmic descriptions. The application is not limited to visualizing the limitations of visually impaired persons, but it also visualizes the effect of myopia and visual limitations due to large viewing distance, eccentric viewing, and low contrast. Our study therefore also gives insight in the limitations of unimpaired subjects and shows how sensitivity to simple test patterns relates to the perception of natural images.

The term 'simulation' may lead to misunderstanding, since it is ill-defined. It may suggest that we seek to visualize how impaired subjects perceive the world. We think that such an undertaking is very difficult, if at all possible. Instead, we will try to visualize the *visual limitations* of impaired subjects. We do not visualize *how* visually impaired persons perceive the world but *what* can be perceived. Our method consists of deforming an image until the difference with the original becomes visible. It comes down to removing from the image visual information that is invisible to the impaired subject. The unimpaired subject that is viewing the simulation is left with the same information, and the simulation therefore gives a good impression of the visual information that is available to the impaired subject. It is well known that viewing strategies can be and are developed by impaired subjects to make optimal use of the remaining visual information. However, this is not subject of our study.

In contrast to so called 'artist impressions' of the perceived scene by impaired subjects we sought to develop a *validated* method of simulation that allows one to make quantitative predictions. By performing human observer experiments we determined what information can be removed from an image before it can be detected. The degree of image degradation reflects the information lost by the impaired subject. As such, this simulation is suitable for evaluating designs, environments (for instance, interior of a public building, road crossings, architecture), and regulations (for instance, for designing stairs).

We developed three types of simulation. The first type, referred to as 'fixation independent', supplies a quick overview into which image elements can be detected and which can not, even when the elements are inspected. Both small elements and elements with low contrast are removed from the image. This simulation is related to object recognition. The second type, referred to as 'fixation

dependent', gives insight into what can be perceived in different (visual) directions while fixating one part of the image. Incorporated into this simulation is the effect that sensitivity for small details decreases with increasing eccentricity. Also the effect of reduced vision due to field defects is taken into account. The third type simulates the effect of glare, an important contributor to low vision in certain types of impairments such as in cataract.

We also determined the relationship between results from standard ophthalmologic tests (acuity, contrast sensitivity, perimetry) and the simulation parameters. With this knowledge it becomes possible to deduce a suitable simulation for an individual from the results from standard tests. Our study also shows how sensitivity to standard test patterns relates to sensitivity to elements in (more complex) natural images for impaired as well as unimpaired persons.

Fixation independent simulation

We performed an experiment in which we determined the amount of just detectable blur in natural images. We investigated whether this can be predicted on the basis of the contrast sensitivity of the subject for standard Landolt-C test patterns, and whether this depends on the type of impairment. We measured contrast sensitivity and blur threshold for different images and for various types of visual impairment. We performed the same measurements with unimpaired persons under various conditions: normal, low contrast, and eccentric viewing, in order to test whether the relationship between acuity and just detectable blur depended on the cause of reduced vision.

Methods

Stimuli

The image was blurred using a blur kernel with width σ, which is equivalent to removing high spatial frequency (SF)-bands. We determined the 75% correct score threshold, corresponding to a value of σ for discriminating the blurred image from the original. Initially, a Gaussian blur kernel was used. However, we noticed that some practiced subjects could subsequently discriminate the images on the basis of low spatial frequency information (certain objects had a different average luminance). To prevent subjects from doing so, we used a difference of Gaussians filter (DOG; with profile given by (2*Gauss(σ) - Gauss($\sqrt{2}$ σ)) instead. This filter keeps the low frequency component unaltered as much as possible and has a steeper fall-off in the spatial frequency domain than a simple Gaussian blur kernel.

Figure 1. The images used in the experiments, referred to as 'face' (a), 'stairs' (b) and 'forest' (c)

Figure 1 shows the three images used in the experiments. The images were tested to determine the effect of image content on the simulation parameters. The images differ in spatial frequency content, for instance, the 'forest'-image contains more high SFs than the other images.

Experimental setup

The images were displayed on a computer monitor (Philips Brilliance low emission 2110), size 37.9 x 28.4 cm or 1024 x 768 pixels at a frame rate of 75 Hz. Calibrated luminance values were used ranging from 0.51 to 174 cd/m^2. A slide projection screen was placed in front of the CRT monitor (40 cm from the monitor) with an aperture the size of the display. The projection screen

was illuminated by two slide projectors, in such a way that a large uniform background around the monitor was created with a luminance that matched the background luminance (87 cd/m^2) of the monitor.

Blur threshold procedure

After the visual acuity of each subject was determined using the method described below, the viewing distance was set to a value that scaled with the minimum angle of resolution (i.e., inversely with acuity) of the subject, such that the viewing distance for a subject with an acuity of 1.0 arcmin^{-1} was 700 cm (for instance, the viewing distance for someone with an acuity of 2.0 is 1400 cm). This relatively large distance was chosen in order that the individual pixels could not be resolved by the subject. This also assured that the number of details that could be discerned in each image was independent of the acuity of the subject.

A Quest adaptive staircase method[3] with a total of 60 trials was used to determine the discrimination threshold (corresponding to a 75% correct score) for blurred images. On each trial the reference and test images appeared side by side, with the order chosen at random. The task to the subject was to indicate the reference image by pressing the mouse button once or twice (reference left or right). The images remained on the monitor until the subject responded. Auditory feedback was given. The measurement program was written in Matlab using the Psychophysics Toolbox extensions[4,5].

Acuity measurement procedure

Acuity of each subject was measured using Landolt-C test symbols, using the same setup as used for measuring the blur threshold (see above). The stimuli were controlled by a Cambridge stimulus generator (VSGcard 2/3-20 MB, maximum luminance of 53 cd/m^2), with a frame rate of 75 Hz. This system allows luminance values to be specified within a 12 bit resolution range. Again, the stimuli were seen through the hole in a slide projection screen, illuminated by four slide projectors, to generate a large uniform background with a luminance that matched that of the CRT.

The minimum angle of resolution (MAR, i.e., 1/acuity) was determined using high contrast Landolt-C patterns (black against a white background) and corresponded to the threshold gap size of the Landolt-C symbol. These thresholds were obtained at similar viewing distances as used for measuring the blur threshold. At each trial one out of four different Landolt-C symbols was shown with the gap to the right, bottom, left, or up. The subject indicated the orientation of the gap by using the joystick. The test pattern remained visible until the subject responded. Auditory feedback was given. A Quest adaptive staircase method[3] was used with 80 trials per staircase to determine the 75% correct threshold values.

Subjects

Ten visually impaired subjects were tested with a range of (combinations of) visual impairments, including macula degeneration, diabetic retinopathy, cataract, and glaucoma. One of the subjects was tested using only one (impaired) eye. The other subjects were tested with both eyes. Age ranged from 58 to 95. We also tested seven visually unimpaired subjects (or corrected to normal) with ages ranging from 22 to 49. Finally, six myopic subjects (ages ranging from 22 to 44) were tested without their correction and after they adapted a few minutes to this situation. We evaluated the effect of reduced contrast with five unimpaired subjects using images that were reduced in contrast by a factor of 0.5, 0.25 and 0.125. Contrast sensitivity for these subjects (with Landolt-C

symbols) was also measured with test patterns in which contrast was reduced by the same factors. Finally, we evaluated the effect of peripheral viewing with three unimpaired subjects that performed the same experiments with fixation 2, 4, and 8 deg in the periphery and a viewing distance of 400 cm (and in one case 500 cm). The fixation point was fixed to the projection screen above the PC monitor. Scaled versions of the face image were used (scaled by a factor of 70% in each dimension) to keep the images at a limited (small) range of eccentricities.

Results

Figure 2a shows the blur threshold (σ) versus the resolution threshold (minimum angle of resolution, MAR), as measured with the Landolt-C test patterns, for different groups of subjects. The blur threshold increases with an increase in the MAR (threshold gap size of the Landolt-C), for instance, the amount of just detectable blur increases with decreasing acuity. Correlation coefficient using all data is 0.92. A least squares fit (linear model) to all (log-) data has a slope of 0.88 +/- 0.04. This is close to the expected value of 1.0 if blur is the only source of reduced vision. Therefore, we will use and test whether the more elegant model with a slope of one describes the data. The average ratio between MAR and blur threshold is equal to 1.94 (with a 95% uncertainty range of 1.78 to 2.11). This means that the blur threshold is about 2 times smaller than the MAR, indicated by the solid line in Figure 2.

The average ratio between MAR and blur threshold is 1.9 (impaired), 2.1 (normal+myopia), 1.6 (reduced contrast) and 2.1 (eccentric), with 95% confidence intervals given by respectively (1.6, 2.3), (1.8, 2.5), (1.5, 1.8), and (1.7, 2.6). Statistical tests (one sided student-t test) show that the values of the ratio of 'normal+myopia' and 'eccentric' are significantly higher than that of the 'reduced contrast' group. The difference between 'impaired' and 'reduced contrast' is close to the significance level ($p = 0.07$). This indicates that the ratio of the 'reduced contrast' data is lower than the ratio of the other data sets. The results further show that the ratio values of all groups except 'reduced contrast' are not significantly different from 2.0.

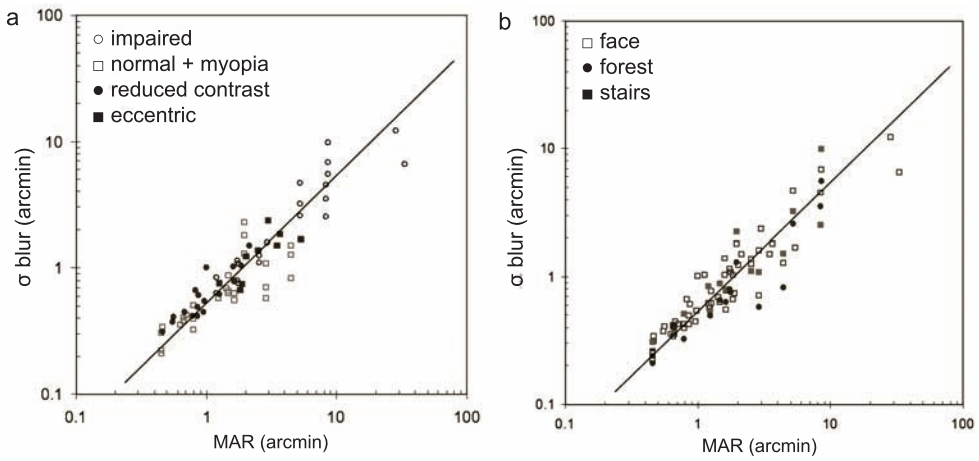

Figure 2. Blur threshold (width of blur kernel σ) versus minimum angle of resolution MAR (= 1/acuity) for the various groups of subjects (a), and for the various types of images (b)

Figure 2b shows the same data, now grouped according to image type. The average ratio between MAR and blur threshold is 1.9 (face), 1.8 (stairs) and 2.4 (forest) with 95% confidence intervals of, respectively, (1.7, 2.1), (1.4, 2.3), and (1.9, 3.0). Pair wise comparison shows that the ratios for the 'face' and 'stairs' image are not significantly different, while the ratio for 'forest' image is significantly higher than the other two. All ratio values are not significantly different from 2.0. The blur threshold for the forest image is significantly lower than that of the other images. This is probably related to the fact that this image contains more high spatial frequencies, which makes a reduction in power more noticable.

Discussion

The main result of this experiment is that the relationship between blur threshold and acuity as measured with Landolt-C symbols is largely independent of the cause of reduced vision, whether due to visual impairment, contrast reduction, or eccentric viewing. Also, the ratio between the MAR and the blur threshold is largely independent of image content. On average the ratio between the MAR and the blur threshold is 2.0, and varies to some (limited) extent from subject to subject. This simple relationship can be taken (as a rule of thumb) to predict how much blur can be introduced in an image before it starts to become noticeable. The fact that this relationship also holds for low contrast images indicates that the contrast sensitivity curve based on orientation discrimination of Landolt-C test patterns is suitable for modelling visibility of elements in natural images.

The fact that the relationship between blur threshold and acuity is the same for low contrast images and for eccentric viewing gives additional support to the idea that this relationship is independent of the type of visual impairment. This is important since many visual impairments lead to a retinal image with lowered contrast (for instance, cataract) while others will be accompanied by the use of eccentric vision (for instance, in case of macular degeneration).

The fact that the blur threshold is inversely proportional to the acuity under various conditions indicates that the visibility of image elements is the same for different subjects and circumstances when the viewing distance is scaled inversely with acuity. Thus, a simple way to estimate which elements can be perceived by a person with lower acuity is by viewing the image from a larger distance, for instance, the same elements are visible for a person with acuity of 0.1 from a distance of 5 m as for a person with acuity of 1.0 from a distance of 50 m!

In first approximation the image can be blurred to an extent that corresponds to the acuity of the simulated subject. Still, the relationship between blur threshold and acuity also holds after a reduction in contrast. This indicates that parts of the image with lower contrast can be blurred even more. The resulting simulation will be a better presentation of the information that can be removed before it becomes noticeable by the impaired subject. A (local) blur can be chosen that varies from location to location in the image depending on the (local) contrast. The link between just noticeable blur and contrast is determined by the contrast sensitivity (the way in which Landolt-C acuity depends on contrast) of the simulated subject.

An unsolved issue is which (local) contrast measure is appropriate. One possibility is to use a localized version of the root-mean-square (RMS) contrast. This measure is equal to the standard deviation (sd) divided by the absolute

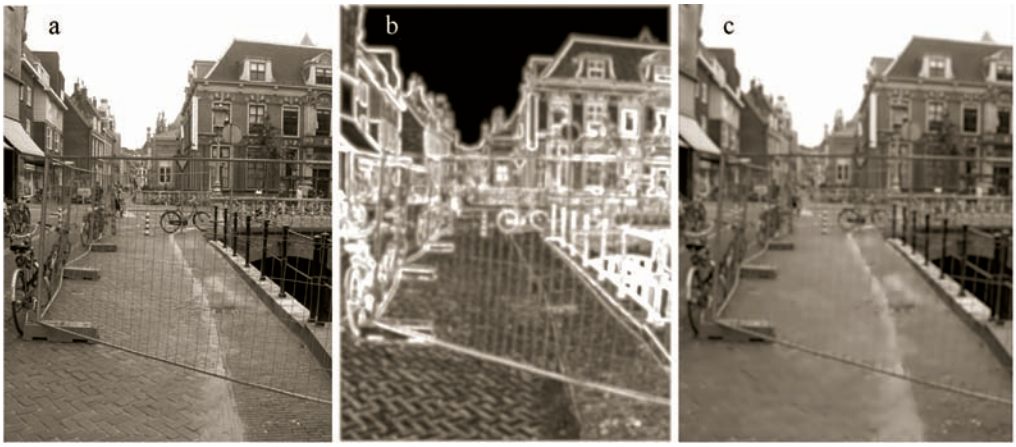

Figure 3. The effect of applying a local blur linked to the local contrast: (a) original image, (b) a measure of local contrast that determines the amount of blur via the contrast sensitivity function, (c) the result of the local blur transformation

value of the average (av): $C = |sd / av|$, in which the standard deviation and average are taken over a local (Gaussian) window. It makes sense to use a window size that scales with the MAR at high contrast. In our simulations we use a window size equal to twice the MAR. Figure 3 shows the result of this transformation. The local average is simply derived from blurring the image with a Gaussian blur kernel. The local standard deviation sd can be derived from the (local) average $\langle x \rangle$ and the (local) average squared value $\langle x^2 \rangle$ using: $sd^2 = \langle x^2 \rangle - \langle x \rangle^2$. Figure 3b shows the local contrast measure deduced for the image shown in Figure 3a. For a given contrast the MAR is derived from the contrast sensitivity function. The amount of just detectable blur is then given by the MAR divided by 2. The result of this transformation is shown in Figure 3c. The effect of the image transformation is that sharp contrast edges remain in the image while regions of low contrast become homogeneous. Between several measures, including Michelson contrast, RMS contrast and average band-limited contrast[6], Bex and Makous[7] found RMS contrast to capture detection of low contrast images best.

Summarizing, our results indicate a clear and simple relationship between acuity as measured with Landolt-C symbols and the amount of just noticeable blur. Based on these results we propose a simulation method in which the local blur adapts to the local contrast.

Fixation dependent simulation

We present a way to simulate reduced vision in the retinal periphery by blurring the image by an amount that depends on the retinal location. The amount of blur is derived from the MAR at that location of the simulated person. For the fixation dependent simulation we used and adapted the implementation developed by Perry and Geisler[8]. They developed an algorithm and software for creating and displaying, in real time, arbitrary variable resolution displays, contingent on the direction of gaze. They demonstrated that the software can be used to simulate the visual fields of normal individuals as well as of low vision patients. They derived the resolution map of low vision patients from Goldman perimeter data as follows. The Goldman perimeter data is used to scale the resolution map of a normal visual field (for a value of -40 dB the resolution is multiplied by 0 and for a value of 0 dB the resolution is multiplied by 1;

personal communication). The normal resolution map is based on a model fit to contrast sensitivity data from Robson and Graham[9] for detecting sinusoidal gratings.

We have found that blur thresholds are well predicted by orientation thresholds for Landolt-C patterns and much less so by detection thresholds for sinusoidal patterns[10]. We propose to use the relationship between acuity and blur threshold to arrive at a simulation of peripheral vision that matches the visibility of elements in natural images. Given the relationship between just noticeable blur and MAR, the (local) blur can be predicted from (local) Landolt-C acuity. Another advantage of coupling the simulation to orientation thresholds of Landolt-C patterns is that this method is commonly used to measure acuity.

As a first approximation we use the resolution map of an unimpaired person and add scotomas, much like Perry and Geisler[8] do, based on the subject's perimeter data. Additionally, we impose the restriction that the minimum amount of blur at each location is in line with the patient's acuity for unrestricted viewing. To arrive at an even more realistic simulation in the future, the link between perimeter data and acuity could be established and incorporated into the simulation[10]; this, however, is not subject of the current study. Here, we show how acuity (measured with Landolt-Cs) varies with eccentricity for unimpaired persons.

Methods

The stimuli were displayed on a PC monitor and consisted of a Landolt-C test pattern displayed in the centre at high contrast, dark on a white background. In the periphery a fixation cross was displayed. The position of the Landolt-C pattern relative to the fixation cross is given by the eccentricity ε and angle φ, representing the angle with the horizontal (for instance, for φ = 90 deg the fixation cross is displayed beneath the Landolt-C pattern). In each session thresholds for a single eye were measured, while the other eye was occluded. The eye was placed in front of the centre of the screen at a fixed distance. The subject's head was stabilised by a chin rest. At each trial a Landolt-C test pattern appeared with the gap in one of eight orientations. The subject indicated the orientation of the gap. An adaptive staircase 8AFC method (QUEST[5]) was used with 50 trials to determine the minimum angle of resolution (MAR) corresponding to a 75% correct score. Two unimpaired subjects participated in the experiment (MAH, NvD). MAR values were obtained for eccentricities of ε = 2, 4, 8, 15 and 30 deg, along directions φ = 180, 225, 270 deg for the right eye (MAH and NvD), and φ = 0, 315, 270 deg for the left eye (NvD). These angles prevent that the test pattern falls into the blind spot. In each session thresholds were obtained for various combinations of eccentricities ε and angles φ. A viewing distance of 60 cm was chosen for eccentricities between 2 and 8 deg, viewing distance of 30 cm for ε = 15 deg, and 20 cm for ε = 30 deg. The PC-monitor was placed on a moving platform. This allowed us to change the viewing distance from condition to condition in random order. All conditions were repeated three times. Shown are geometric averages over all conditions.

Results

Figure 4 shows the thresholds as a function of eccentricity for angular directions (φ) for each eye, along with the data from experiment 1, obtained with a different setup. In the first experiment the relationship between blur threshold and MAR was established. In the second experiment a different, for this purpose more convenient, setup was used to measure acuity in the periphery. To estimate the blur threshold for a given ret-

inal location it is necessary to determine whether and how the different method and setup affected the results. The experiments differed in a number of ways. First, in experiment 2 an 8AFC method was used to arrive at stable threshold results with fewer measurements. Second, the data were obtained with a single eye instead of with both eyes. Also, a much shorter viewing distance was used in the second experiment. The thresholds obtained here differ on average by a factor of 1.5 (MAH: 1.50; NvD: 1.55) from those obtained in the first experiment. In a control experiment with a single subject (NvD) the effect of using an 8AFC-method instead of a 4AFC-method was investigated[10]. This showed that using a 4AFC procedure the thresholds were still about 1.3 times higher than in the first experiment. This is likely due to the fact that here a single eye is used instead of two. We measured MAR values of 0.66 arcmin (MAH) and 0.47 arcmin (NvD) in the main experiment (central fixation, two eyes). Thresholds measured here were 1.5 (MAH) and 1.55 (NvD) times larger, and therefore correspond to the eccentric acuity curve of a person with central acuity of 1.5*0.66 = 1.0 (MAH) and 1.55*0.47 = 0.73 arcmin (NvD). To model eccentric acuity of a person with central acuity of 1 arcmin we therefore fitted a 2nd order polynomial fit (minimizing the log-differences) to the data of the right eye of subjects MAH and NvD*1.4 (=1/0.73). This model curve is shown in Figure 4a. The model corresponds to the acuity of a person with central acuity of 1.0. The following equation describes the relationship between acuity (=1/*MAR*) and eccentricity (ε):

$$MAR(\varepsilon) = a\varepsilon^2 + b\varepsilon + c, \qquad (1)$$

in which a = 0.01, b = 0.67 and c = 1. Since the acuity of the right eye of subject MAH is 1.5 times the acuity of both eyes in the first setup, being 1, this happens to coincide with the thresholds of the right eye of subject MAH.

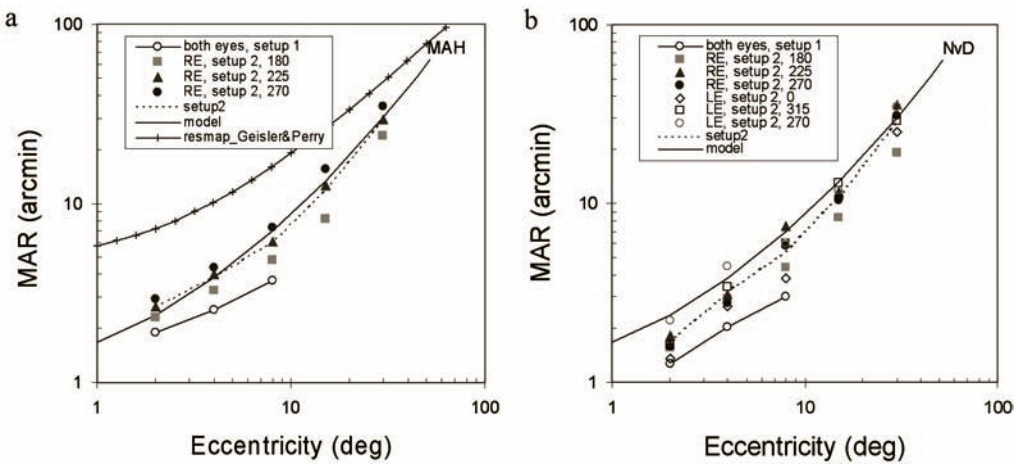

Figure 4. MAR as a function of eccentricity for the two subjects, for different angles (φ) and eyes (right = RE, left = LE); the dotted line represents the average over all values. Also shown are the thresholds from the fixation independent experiment (setup 1); the drawn line represents the model for an unimpaired subject with acuity of 1.0. This (accidentally) coincides with the right eye data of subject MAH, but is higher than the data of subject NvD. Also, shown with subject MAH, is the standard model used in the visual field simulator of Perry and Geissler[8]

Figure 5. Comparing different resolution models of unimpaired subjects; result of the transformation method based on the Perry and Geisler[8] model (a), and the result of our model derived from Landolt-C acuity (b); the image spans a visual field of 54 x 42 degrees

Discussion

We use the Visual Field Simulator[8,11] to model eccentric viewing. We make use of the 'space variant imaging-toolbox' developed by Geisler and Perry[12]. The resolution map describes the way in which the resolution varies across the retina. Perry and Geisler use a resolution map for unimpaired persons based on a model fitted to the data from Robson and Graham[9] corresponding to detection of sinusoids. We have found that contrast sensitivity based on orientation discrimination of Landolt-Cs accurately describes sensitivity to blur in natural images. Therefore, we use a resolution map derived from the Landolt-C acuity data obtained in the periphery.

The resolution map is derived as follows. First, for each pixel the eccentricity is calculated. Then equation (1) is used to derive the MAR for each pixel. Next, the relationship between MAR and just detectable blur (section 2) is used to deduce the blur threshold. The ratio between the MAR and the width of the (Gaussian) blur threshold (σ) is 2.0. So, to arrive at the amount of (Gaussian) blur σ for each pixel the MAR is divided by 2. Finally we deduce the resolution from the blur threshold, in which the resolution as used in the Visual Field Simulator corresponds to 0.6418 / σ (personal communication with Dr. Perry). For this value of the resolution parameter, the point at which the attenuation factor equals 0.5 is equal for the Visual Field Simulator and a Gaussian blur kernel.

Using the same formula the predicted MAR can be deduced from the resolution map. This has been done for the standard resolution map used in the Visual Field Simulator. The model is shown in Figure 4a. The MAR predicted by this model is much higher than the measured threshold data, especially for low eccentricities.

Figure 5 shows a transformed image covering an angle of 54 x 42 deg (with fixation at the centre). Figure 5a shows the result using the standard resolution map proposed by Perry and Geisler[8]. Figure 5b shows the result derived from the acuity thresholds for Landolt-Cs. Both models describe the peripheral resolution of an unimpaired subject. The area around the fixation point for which there is no blur is much larger in the latter case. For larger eccentricities the resolution falls off more rapidly, and for large eccentricities the resolution is about the same for the two models (Figure 4a).

The resolution map of low vision patients can be deduced from the normal

resolution map using the same method as followed by Perry and Geisler[8], or by simply adding the scotomas. To arrive at an improved simulation we use the extra restriction that the minimum resolution of the resolution map can not be lower than the one derived from acuity during free viewing.

This simulation is based on our findings that the amount of detectable blur is directly linked to the Landolt-C acuity and that this relationship is independent of the cause of reduced acuity (including peripheral viewing, at least for eccentricities up to 8 deg). Whether this assumption is true should be the subject of further testing.

Simulating glare

Disability glare is glare that impairs vision. It is largely caused by scattering of light inside the eye because of the imperfect transparency of the optical components of the eye. It results in a kind of veiling luminance. Our simulation of this phenomenon is based on validated formulas[13] describing the relationship between the veiling luminance and the luminance of the light source and the angle between the viewing direction and the light source. We add a veiling luminance that varies over the image. We start with an image of luminance values. We then calculate the contribution to the veiling luminance resulting from any other pixel, for instance the other pixel is regarded as the light source causing the veiling luminance. The total veiling luminance for any given pixel is calculated by summing over the contribution of all other pixels.

The contribution of each pixel to the veiling luminance is calculated using the equation describing the illuminance *dE* resulting from a light source with luminance *L* spanning an angle α:

$$dE = L^{*}d\alpha \quad (2)$$

Each light source causes a veiling luminance described by CIE General Disability Glare equation[13]:

$$\frac{L_{veil}}{E_{glare}} = \frac{10}{\theta^3} + \left[\frac{5}{\theta^2} + \frac{0.1p}{\theta}\right] \cdot \left[1 + \left(\frac{Age}{62.5}\right)^4\right] + 0.0025p \quad (3)$$

in which *p* represents the *eye pigmentation factor* (0 for black, 0.5 for brown, 1 for light and 1.2 for very light eyes). This formula is valid for angles θ between 0.1 en 100 deg.

The formula shows that the disability glare rapidly increases with an increase in age. For an age of 62.5 years the second term is twice as large. A good approximation for angles θ between 1 and 30 deg is given by:

$$\frac{L_{veil}}{E_{glare}} = \frac{10}{\theta^2} \cdot \left[1 + \left(\frac{Age}{70}\right)^4\right] \quad (4)$$

This equation is the so called CIE Age-adjusted Stiles-Holladay Disability Glare equation. This veiling luminance can be multiplied by a factor κ that depends on the amount of light scatter in someone's eye. For cataract patients κ lies between 2 and 8[14]:

$$\frac{L_{veil}}{E_{glare}} = \frac{10}{\theta^2} \cdot \kappa \quad (5)$$

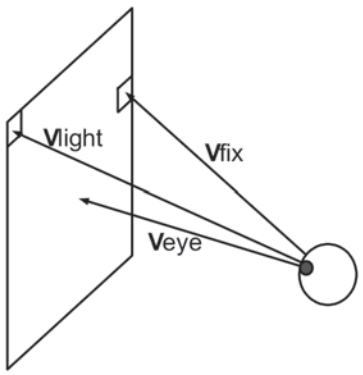

Figure 6. Schematic representation of the vectors involved in the calculation of the veiling luminance: the normal vector connecting the centre of the screen with the eye ($\mathbf{V}_{eye}$), the fixation point ($\mathbf{V}_{fix}$), and the position of the light source ($\mathbf{V}_{light}$)

Figure 7. Example of disability glare; (a) original image; (b) transformed image to which a veiling luminance is added for a glare factor of $\kappa = 8$

In the simulation for each pixel we assume that the subject fixates one pixel and we calculate the veiling luminance for this pixel by summing over the veiling luminance contribution of all other pixels using equations (5) and (2).

Figure 6 shows the vectors involved in the calculation. For each fixation point ($\mathbf{V}_{fix}$) the contribution to the veiling luminance of each other pixel ($\mathbf{V}_{light}$) is calculated and summed. The illuminance E_{glare} of this light source is calculated from the luminance of the pixel and the viewing angle (which follows from the pixel area and the angle between eye and light vector), using equation (2). Next, equation (5) is used to calculate the veiling contribution from this light source to the fixated pixel. The angle θ equals the angle between the fixation ($\mathbf{V}_{fix}$) and the light vector ($\mathbf{V}_{light}$). The contribution of all pixels is summed, and the calculations are repeated for all pixels.

Figure 7b shows the result of the glare simulation with $\kappa = 8$ applied to Figure 7a. Since the luminance values are unknown, assumptions have to be made about the conversion of luminance values (L) to pixel (x) values (as well as the conversion on the display). Commonly used is a gamma function ($L = x^{\gamma}$, with a γ of around 2). In some cases the calibrated luminance values will be available and can be used to obtain a more realistic simulation (for instance, in a virtual design resulting from ray tracing techniques).

This simulation is based on the standard CIE (validated) model of glare[13], derived from human observer experiments with a single light source. Our model extends this model to an array of light sources. Given that the veiling luminance is largely due to scatter in the eye it seems plausible that the individual contributions of the various light sources can simply be summed as our model does. Therefore, we expect that the simulation gives an accurate description of the perceived veiling luminance. Whether this is indeed the case can be tested by performing experiments in which various image elements should be detected, and comparing this to the model predictions.

General conclusion

To goal of this study was to find and implement ways to visualize the limitations of visually impaired persons. We implemented three types of simulations: (i) fixation independent, (ii) fixation dependent, and (iii) the effect of glare. The first type shows the information that is available when a person inspects the scene with his or her best part of the visual field. The simulation shows which elements are and which are not visible when attention is fo-

cused on that part of the scene. As such, the simulation is related to human performance for recognising objects. The second type shows the information that is available everywhere in the visual field when a person fixates a particular part of the scene. This simulation gives insight into visual search for an item, for instance the simulation is related to the conspicuity of elements in the scene. It also shows which information is available when the time to inspect a scene is short. Since simulations (i) and (ii) give insight into other aspects of visual processing (object recognition vs. object detection) they both are valuable simulations, and depending on the task one or the other will be more suitable.

An experiment with impaired and unimpaired subjects was performed that showed a simple relationship between acuity and amount of just noticable blur. Moreover, this relationship was found to be largely independent of the cause of reduced vision (visual impairment, low contrast, eccentric viewing). The fact that this relationship holds for low contrast images indicates that a contrast sensitivity curve based on discrimination of Landolt-C symbols is appropriate for modelling visual limitations. Based on this finding we propose a fixation independent simulation in which the (local) blur adapts to the (local) contrast. This comes down to a direct (local) implementation of the relationship between amount of just detectable blur and the acuity (at that contrast level).

The relationship between acuity and just detectable blur in natural images is also used to model the fixation dependent simulation. The simulation method is based on the assumption that the relationship between just detectable blur and Landolt-C acuity is independent of eccentricity (as found in the main experiment) and also holds for eccentricities larger than 8 deg (the maximum eccentricity used in the main experiment). We measured Landolt-C acuity in the peripery and from this we deduced a model describing the acuity of an (unimpaired) subject with acuity of 1.0. The relationship between blur threshold and acuity is then used to derive a model of the just detectable blur in the periphery of an unimpaired subject. The resolution map of an impaired subject is then deduced from the resolution of an unimpaired subject, the perimeter data of the subject, and the central acuity of the subject (imposing a lower resolution limit). It is clear that in regions with an absolute scotoma the subject is not able to perceive anything. It is still unclear what the blur threshold is in regions in which there are relative scotomas (i.e., where there is reduced vision). In a future study the relationship between the perimeter results and blur thresholds should be established. Still, the simulation will be correct in many respects (for instance, regarding the minimum acuity, minimum decrease in acuity with eccentricity, absolute scotomas).

We also investigated ways to simulate the effect of glare, since for certain types of impairments this has a big impact (for instance, cataract). For this simulation we resorted to well-validated CIE equations[13]. A veiling luminance is calculated for each part of the image that results from the light originating from other parts of this image. The veiling luminance is therefore representative for the situation that an observer looks at that part of the image. This simulation can also be used in combination (as a first step) with the fixation independent and fixation dependent simulations.

The simulations described in this study are implemented in software[15] . This tool allows one to degrade an image such that it visualizes which information

is available to a low vision patient using the patient's results from ophthalmologic tests (acuity, perimetry, and light scattering data). The idea is that by using this tool, people with normal vision gain more understanding of the abilities and inabilities of visually impaired persons. The hope is that this will (eventually) lead to an environment that is better adapted to the needs, abilities and limitations of visually impaired persons.

Acknowledgements

This work was funded by InZicht via NWO/ZonMw. We wish to thank our collaborators Dr. I.T.C. Hooge, and B.P.L.M. den Brinker for their contributions and helpful discussions and Prof. Dr. G.H.M.B. van Rens, Ir. F.F. Jorritsma and T. Blom for their corporation and help in setting up the experiments with low vision subjects. We also very much appreciate the effort, work and discussions with trainees from the University of Utrecht, J. van Elst, N. Boogaards and N. van Dijk, who conducted many of the experiments. We would also like to thank the students E.J.L. Brunenberg, H.J. Buisman, W.L. de Graaf, J.W. van Triest and J. Uittenbogaard from Technische Universiteit Eindhoven (Department of Biomedical Engineering) and their supervisor Dr. L.M.J. Florack for their contribution to the development of a useful image transformation method. We thank Dr. Geisler and Dr. Perry for using their software and help in developing the simulation software.

References

1. Gill J. Keeping step. London: Royal National Institute for the Blind Scientific Research Unit; 2001
2. Walraven J, Alferdinck JWAM. Color displays for the color blind. Proceedings of the 5th Color Imaging Conference, Color Science, Systems, and Applications, November 17-20, 17-22. Scottsdale, Arizona; 1997
3. Watson AB, Pelli DG. QUEST: a Bayesian adaptive psychometric method. Perception and Psychophysics 1983;33(2):113-120
4. Brainard DH. The Psychophysics Toolbox. Spatial Vision 1997;10:433-436
5. Pelli DG. The VideoToolbox software for visual psychophysics: Transforming numbers into movies. Spatial Vision 1997;10:437-442
6. Peli E. Contrast in complex images. Journal of the Optical Society of America A. 1990;7:2032-2040
7. Bex P, Makous W. Spatial frequency, phase, and the contrast of natural images. Journal of the Optical Society of America A. 2002;19:1096-1106
8. Perry JS, Geisler WS. Gaze-contingent real-time simulation of arbitrary visual fields. In: Rogowitz BE, Pappas TN, editors. Human Vision and Electronic Imaging VII, San Jose: SPIE Proceedings; 2002;4662:57-69
9. Robson JG, Graham N. Probability summation and regional variation in contrast sensitivity across the visual field. Vision Research 1981;21:409-418
10. Hogervorst MA, van Damme WJM. Visualizing visual impairments. Soesterberg: TNO report; 2006; www.sensis.nl; Retrieved August 30, 2006
11. Geisler WS, Perry JS. A real-time foveated multiresolution system for low bandwidth video communication. SPIE Proceedings: Human Vision and Electronic Imaging 1998;3299:294-305
12. Geisler WS, Perry JS. Space variant imaging software: 2005; http://svi.cps.utexas.edu/svitoolboxdoc/svitoolbox/Contents.html; retrieved August 30, 2006
13. CIE. CIE equations for disability glare, Commission Internationale de l'Éclairage (CIE), Vienna: CIE 146 ; 2002
14. de Waard PW, IJspeert JK, van den Berg TJ, de Jong PT. Intraocular light scattering in age-related cataracts. Investigative Ophthalmology and Visual Science 1992;33(3):618-625
15. Low-vision simulator, including manual and background; www.sensis.nl; retrieved August 30, 2006